REPORT NO. 32
January, 1950

THE COLLEGE OF AERONAUTICS

CRANFIELD

An Empirical Method for Rapidly Estimating the Loading Distributions on Swept Back Wings

-by-

R. Stanton Jones, B.A. (Hons.Cantab.), D.C.Ae.

SUMMARY

This paper describes the derivation of empirical formulae for the loading distribution on straight tapered swept back wings, in terms of the parameters governing the geometric wing plan form. The derivation is based mainly on the results of the Weissinger method but corrections to give better agreement with experimental results have been introduced.

The method depends entirely on the assumption that the shape of the loading curve can be completely defined by the position of the spanwise centre of pressure ($\bar{y}$). Although this assumption cannot be backed theoretically the analysis shows that there is plenty of sound evidence to support it.

The shape of the loading curve is then shown to be expressible explicitly in a formula involving $\bar{y}$. This formula can be used to derive the loading distribution for any particular wing falling within a wide range of aspect ratio, taper ratio, and sweepback angle, and the calculation can be completed in a matter of minutes to an accuracy comparable with that of the Falkner method. In addition, the method allows the results of the linear perturbation theory of compressible flow to be easily incorporated. However, it suffers from the limitation that it applies only to simple trapezoidal wing plan forms.

The formulae are -

The location of the Spanwise Centre of Pressure in incompressible flow

$$\bar{y} = .42 + \frac{A}{10^3}\left[(4.4 + 5\lambda)\tan\Gamma + 10.4\lambda^{\frac{1}{2}} - 6.7\right]. \quad \ldots\ldots\ldots (1$$

The Non-Dimensional Loading Coefficient at the Spanwise Station - η

$$\left(\frac{\partial C_L}{\partial \bar{C}_L}\right)_\eta = 1.28\,(1-\eta^2)^{\frac{1}{2}} + \begin{bmatrix} (-6.35 + 14.13\eta)_{\eta \leq .7} \\ 4.25 - 53.8\,(\eta - .815^2)_{\eta \geq .7} \end{bmatrix}\left[\bar{y} - .425\right] \quad \ldots (1$$

The location of the Spanwise Centre of Pressure in incompressible flow

$$\bar{y} = .42 + \frac{A_M}{10^3}\left[(4.4 + 5\lambda)\tan\Gamma_M + (10.4\lambda^{\frac{1}{2}} - 6.7)\sqrt{1 - M^2}\right] \ldots (1$$

DMSJ

NOTATION

Γ = sweepback of the 1/4 chord line

A = aspect ratio

λ = taper ratio $\frac{\text{tip chord}}{\text{root chord}}$

$b/2$ = semi-span

η = spanwise position/semi span

$\bar{c}$ = geometric mean chord

$\bar{C}_L$ = mean lift coefficient for whole wing

$\bar{y}$ = spanwise position of centre of pressure

K_λ = slope of $\left(\frac{\partial \bar{y}}{\partial A}\right).\sim.\tan\Gamma$ lines

B_λ = intercepts of $\left(\frac{\partial \bar{y}}{\partial A}\right).\sim.\tan\Gamma$ lines on the $\left(\frac{\partial \bar{y}}{\partial A}\right)$ axis

K_η = loading coefficient $\frac{cC_L}{\bar{c}\bar{C}_L}$

Q_η = slope of $K_\eta.\sim.\bar{y}$ lines

A_M = aspect ratio for wing at Mach number M

Γ_M = sweepback angle for wing at Mach number M

---

1. Introduction

For a wing of any given plan form there are a number of methods for determining the loading distribution and among the better known are those due to Falkner[13-39,72-74], Multhopp, Weissinger[1], and more recently Schlichting and Thomas[43]. However, all these methods involve quite a considerable amount of computing work and time and do not readily present a general picture of the relative effects of sweepback, aspect ratio or taper ratio on the shape of the loading curve. It was decided, therefore, to develop a semi-empirical approach based on the results obtained by applying one of these analytical methods modified in the light of such actual experimental evidence as was available. The ultimate object was the development of a method that would be both quick to apply and would readily demonstrate the part played by the various geometrical and aerodynamic parameters in controlling the loading distribution.

The resulting method presented here applies to straight tapered swept back wings and appears to give results that are satisfactory for most practical purposes, whilst the time of computation involved in any particular case is of the order of a few minutes.

2. The Weissinger method (Reference 1)

The Weissinger method replaces the spanwise load by a line vortex at the 1/4 chord position. The spanwise strength variation of this vortex is determined by the boundary condition that there can be no flow through the mean camber line at the 3/4 chord point. This is exactly the same set of assumptions as those adopted by Multhopp who attempted an analytical treatment of the resulting series. However, Weissinger preferred to determine the circulation directly at four spanwise points.

The theory is applicable to all plan forms, including those which have camber and twist. Nevertheless, it is usual to consider the loading in two parts, viz., the 'basic loading'[R] due to camber and twist at zero total lift and the 'additional loading' due to angle of attack. Only the 'additional loading' will be considered here.

/3. ...

[R] An empirical method for the basic loading is in the course of preparation.

3. Range of aerofoils considered

In Reference 6 the Weissinger method has been applied to straight tapered wings within the following range.-

Aspect ratio range	1.5 to 8
Sweep back range	0° to 60°
Taper ratio range	0 to 1.5

Wings with five taper ratios were considered. They were -

$$\lambda = 0,\ .25,\ .5,\ 1.0,\ \text{and}\ 1.5.$$

For each of these taper ratios graphs were drawn of -

(a) the variation of the spanwise centre of pressure $\bar{y}$, with sweepback angle Γ for each aspect ratio A. (A typical set for $\lambda = .5$ is shown in Fig.1).

(b) The variation of the spanwise loading coefficient $\left[\frac{cC_L}{\bar{c}\bar{C}_L}\right]$ with sweepback for each A at the four spanwise positions -

$$\eta = 0,\ .3827,\ .7071,\ \text{and}\ .9239.$$

4. Loading curve shape parameter

From the curves (a) cross plots were obtained of A versus Γ for various spanwise centre of pressure positions $\bar{y}$, at each of the taper ratios λ. (A typical set for $\lambda = .5$ is shown in Fig.2). These $A \sim \Gamma$ lines were then used in conjunction with the graphs (b), and the loading curves $\left[\frac{cC_L}{\bar{c}\bar{C}_L}\right]$ against η were derived for various wings whose geometric shapes are defined by Γ, A, λ, for constant values of $\bar{y}$. The process was applied to numerous values of $\bar{y}$ from $\bar{y} = .415$ to .480. (See Fig.3 for a typical set of results).

In every case it was found that all wings (Γ, A, λ) which had the same spanwise centre of pressure position, $\bar{y}$, had practically the same non-dimensional spanwise loading curve $\left[\frac{cC_L}{\bar{c}\bar{C}_L}\right] \sim \eta$. Hence, all the wings which form the locus of any one of the $A \sim \Gamma$ lines (such as in Fig.2) have a loading curve whose shape may be entirely defined by $\bar{y}$.

/The ...

The loading curves which have been drawn to illustrate this result in each case (e.g. Fig.3) have been taken from the extreme limits of the $\Lambda \sim \Gamma$ lines, and the discrepancies between the loadings represent the maximum discrepancies that occur for wings of similar $\bar{y}$ within the range considered.

The worst discrepancy encountered was only found to be of the order of 2 per cent which compares favourably with the sort of accuracy to which experimental readings of pressure plots may be made.

On the basis of this analysis it was decided to accept $\bar{y}$ as the loading curve shape parameter.

5. $\bar{y} \sim \Lambda$ relation

The problem now reduces itself into the empirical solution of the equation

$$\bar{y} = f(\Gamma, \Lambda, \lambda). \qquad \ldots\ldots\ldots\ldots\ldots\ldots (1)$$

Cross plotting from the $\Gamma \sim \Lambda$ lines we next obtain the set of curves $\bar{y}$ against Λ for various Γ at each λ. A typical set for $\lambda = .5$ is shown in Fig.4. It can be seen that these $\bar{y} \sim \Lambda$ curves are all not far off straight lines. We therefore assume that the $\bar{y} \sim \Lambda$ curves may all be represented by straight lines which pass through the point .42 on the $\bar{y}$ axis. The cases where the assumption is clearly weak fall outside normal practical bounds. Thus we note that.-

1. wings with $\lambda = 0$ are not likely to be met with when $\Gamma = 0$ if Λ is above about 4.0.

2. Wings with λ between .5 and 1.0 are not frequently used when Γ is low and Λ is below about 2.0, or when Γ is high and Λ is also high.

We may also note that the Weissinger method is known to underestimate the load at the tips. We can, therefore, expect values of $\bar{y}$ to be slightly greater than those derived from the Weissinger method.

6. Relations between $\bar{y}$, Λ, Γ and λ

Using the straight line representation of the $\bar{y} \sim \Lambda$ curves we now obtain their slopes for every value of Γ considered at each taper ratio (see Table I). Thus,

$$\bar{y} = \bar{y}_\lambda + \left(\frac{\partial \bar{y}}{\partial \Lambda}\right)_{\Gamma,\lambda} \Lambda, \qquad \ldots\ldots\ldots\ldots\ldots\ldots (2)$$

where $\bar{y}_\lambda = .42$ for all λ.

/Plotting ...

Plotting these slopes $\left(\frac{\partial \bar{y}}{\partial \Lambda}\right)_{\Gamma,\lambda}$ against $[\tan \Gamma]$ we obtain Fig.3 which suggests that we may reasonably draw straight lines through the points obtained for any one taper ratio λ. The points obtained for $\lambda = 0$ do not lend themselves to this simplification as readily as the points obtained for the other taper ratios. The equations of those straight lines (Fig.5) may be generally expressed by

$$\left(\frac{\partial \bar{y}}{\partial \Lambda}\right)_{\lambda} = K_{\lambda} \tan \Gamma + B_{\lambda} \qquad \ldots\ldots\ldots\ldots\ldots\ldots (3)$$

where K_{λ} is the slope at a particular taper ratio λ and B_{λ} is the intercept on the $\left(\frac{\partial \bar{y}}{\partial \Lambda}\right)$ axis. Thus the individual equations become

$$\left(\frac{\partial \bar{y}}{\partial \Lambda}\right)_{0} = .0025 \tan \Gamma - .0065. \qquad \ldots\ldots\ldots\ldots\ldots\ldots (4)$$

$$\left(\frac{\partial \bar{y}}{\partial \Lambda}\right)_{.25} = .00575 \tan \Gamma - .0015. \qquad \ldots\ldots\ldots\ldots\ldots\ldots (5)$$

$$\left(\frac{\partial \bar{y}}{\partial \Lambda}\right)_{.5} = .0067 \tan \Gamma + .0008. \qquad \ldots\ldots\ldots\ldots\ldots\ldots (6)$$

$$\left(\frac{\partial \bar{y}}{\partial \Lambda}\right)_{1.0} = .0093 \tan \Gamma + .00375. \qquad \ldots\ldots\ldots\ldots\ldots\ldots (7)$$

$$\left(\frac{\partial \bar{y}}{\partial \Lambda}\right)_{1.5} = .0119 \tan \Gamma + .0060. \qquad \ldots\ldots\ldots\ldots\ldots\ldots (8)$$

Plots of K_{λ} against λ, and B_{λ} against λ and $\lambda^{\frac{1}{2}}$ (see Fig.6) now lead to the equations

$$K_{\lambda} = .0044 + .005\lambda. \qquad \ldots\ldots\ldots\ldots\ldots\ldots (9)$$

and

$$B_{\lambda} = -.0067 + .0104\lambda^{\frac{1}{2}}. \qquad \ldots\ldots\ldots\ldots\ldots\ldots (10)$$

Thus, substituting in the equation for $\left(\frac{\partial \bar{y}}{\partial \Lambda}\right)_{\lambda}$ we have

$$\left(\frac{\partial \bar{y}}{\partial \Lambda}\right)_{\lambda} = (.0044 + .005\lambda) \tan \Gamma - .0067 + .0104\lambda^{\frac{1}{2}}. \qquad \ldots\ldots\ldots\ldots\ldots\ldots (11)$$

Put $\bar{y} = .42 + \left(\frac{\partial \bar{y}}{\partial \Lambda}\right)_{\lambda} \Lambda.$ $\ldots\ldots\ldots\ldots (2)$

Thus $\bar{y} = .42 + \frac{\Lambda}{10^3}\left[(.4 + 5\lambda) \tan \Gamma + 10.4\lambda^{\frac{1}{2}} - 6.7\right]$ $\ldots\ldots\ldots\ldots\ldots\ldots (12)$

/This ...

This is the final formula which is the parametric relationship between the geometric shape of the aerofoil and the shape of the non-dimensional loading curve.

7. The accuracy of the empirical formula

The process of derivation of this formula is undoubtedly crude but its results can be readily checked against the initial data and its accuracy can be assessed insofar as one accepts the accuracy of the initial data. This was done for some forty different wings, covering the entire range of aerofoils considered, and the comparisons between the original Weissinger results for $\bar{y}$ and the results obtained by means of the empirical formula are shown in Table II.

In the majority of cases the empirical formula gives results which are slightly larger than the Weissinger values but this was implicit in our assumptions and deliberately introduced to allow for the fact that the Weissinger method appears to underestimate $\bar{y}$ slightly in certain cases.

In the few instances where the empirical formula underestimates the value of $\bar{y}$ the difference is small.

8. The suitability and importance of $\bar{y}$ parameter

There is some doubt as to the suitability of $\bar{y}$ as a parameter, mainly because its total variation is only from about .400 to .500, and in this range a wide variation of wing plan form is possible, from a triangular slightly swept wing of low aspect ratio to a rectangular highly swept wing of large aspect ratio.

However, the empirical formula appears to be capable of estimating $\bar{y}$ to within .003 (see Table II), which represents 3 per cent of the total $\bar{y}$ range, while an error of .003 in estimating $\bar{y}$ only corresponds to an approximate error of 3° in the angle of sweepback. Thus the formula might be considered as accurate enough for most purposes.

9. Shape of the loading curve

Now that we have obtained a value of $\bar{y}$ which may be readily computed for any wing, we require to relate $\bar{y}$ to the actual shape of the loading curve and so relate the loading curve to the parameters governing the geometric layout of any wing. The shapes of the loading curves used were derived from Reference 6; they represent the actual Weissinger results and no attempt has been made to correct them to fit experimental curves.

/Reference ...

Reference 6 only considers four spanwise stations but from the mean curves of loading distributions (e.g. Fig.3) the loading coefficient $K_\eta = \left[\frac{cC_L}{\bar{c}\bar{C}_L}\right]$ was determined at ten spanwise positions for seven types of loading (i.e., for seven values of $\bar{y}$).

If K_η, the loading coefficient, is now plotted against $\bar{y}$ for each of the ten spanwise positions considered, we obtain points that may easily be represented by a set of straight lines (see Figs. 7 and 8).

It may be shown that the value of $\bar{y}$ for elliptic loading is very close to .425. Thus, if the K_η axis is taken at $\bar{y} = .425$ in Figs. 7 and 8, the intercepts of the $K_\eta \sim \bar{y}$ lines on this axis should give an ellipse when plotted out against η. It was found that this was almost exactly true. We shall therefore take the K_η axis as passing through $\bar{y} = .425$ and this defines a fundamental loading curve.

The $K_\eta \sim \bar{y}$ lines may be represented by the general equation

$$K_\eta = K_{\bar{y}} + Q_\eta (\bar{y} - .425) \qquad \ldots\ldots\ldots\ldots (13)$$

where $K_{\bar{y}}$ is the intercept of the lines on the K_η axis and Q_η is the slope $\left[\frac{\partial K_\eta}{\partial \bar{y}}\right]_\eta$.

We have already discovered that the variation of $K_{\bar{y}}$ with η is very nearly elliptical and it may be written

$$K_{\bar{y}} = 1.28 (1 - \eta^2)^{\frac{1}{2}}. \qquad \ldots\ldots\ldots\ldots (14)$$

The slopes Q_η are shown in Table IV and plotted in Fig.9 where it may be seen that they form a straight line from $\eta = 0$ to $\eta = .7$, but thereafter the curve appears to be parabolic. Hence, we find Q_η is very closely given by

$$Q_\eta = \left[\begin{array}{l} (-6.35 + 14.13\,\eta)_{\eta \leq .7} \\ \left\{4.25 - 53.8\,(\eta - .815)^2\right\}_{\eta \geq .7} \end{array}\right]. \qquad \ldots\ldots (15)$$

/Substituting ...

Substituting for $K_{\bar{y}}$ and Q_η the complete loading formula becomes -

$$\frac{c_L}{\bar{c}_L} = 1.28\,(1-\eta^2)^{\frac{1}{2}} + \begin{bmatrix} (-6.35 + 14.13\,\eta)_{\eta \leq .7} \\ 4.25 - 53.8\,(\eta - .815)^2 \quad _{\eta > .7} \end{bmatrix} \left[\bar{y} - .425\right] \quad . (16)$$

where $\bar{y}$ may be calculated bynthe empirical formula already given[*].

10. Accuracy of the loading formula

For $\bar{y} = .44$ we have the following comparison.-

η	Empirical formula	Weissinger
0	1.185	1.185
.383	1.168	1.160
.707	.959	.955
.923	.551	.555

This agreement is typical. Thus, providing the value of $\bar{y}$ is correct this empirical formula allows us to reproduce almost exactly the corresponding Weissinger loading curve.

We have already noted that $\bar{y}$ may be in error by approximately .003 and it is found that the maximum error in $\left[\frac{c_L}{\bar{c}_L}\right]$ which this is likely to cause is just over 1 per cent from the mean Weissinger value. This is within the originally estimated maximum difference between loading curves with identical $\bar{y}$ values (i.e., 2 per cent maximum difference). However, it should be remembered that Weissinger loading curves do not always agree with experimental results and no allowance has been made for this fact except in the estimation of $\bar{y}$.

11. Collected formulae

The loading distribution on any straight tapered swept back wing may be derived with an accuracy suitable for most practical purposes by the application of the following formulae.

/(formulae) ...

---

[*] Once $\bar{y}$ is obtained, values of $\frac{c_L}{\bar{c}_L}$ may be read directly from the $K_\eta . \sim . \bar{y}$ lines Figs. 7 and 8. The formula is mainly of use where partial areas of the loading curve are required, e.g., for bending moments.

$$\bar{y} = .42 + \frac{A}{10^3}\left[(4.4 + 5\lambda)\tan\Gamma + 10.4\lambda^{\frac{1}{2}} - 6.7\right] \quad \ldots(15)$$

$$\frac{dC_L}{d\bar{C}_L} = 1.28\,(1-\eta^2)^{\frac{1}{2}} + \begin{cases} (-6.35 + 14.13\eta)_{\eta \leq .7} \\ 4.25 - 53.8\,(\eta - .815)^2_{\eta \geq .7} \end{cases} \left|\bar{y} - .4\right| \ldots$$

$$\ldots\ldots(16)$$

$\frac{dC_L}{d\bar{C}_L}$ may also be obtained by reading directly from the $K_\eta . \sim . \bar{y}$ lines (Figs. 7 and 8).

12. Comparison with experimental results and Falkner's calculation

A comparison between the loading curves obtained by the empirical method suggested above and an experimental pressure plot are shown in Fig.10. (Reference 8).

The wing has $A = 7.51$, $\Gamma = 23^\circ$ and $\lambda = .243$, and there is reasonable agreement except at the root. A comparison with the results of Falkner's calculation was made for the following wings. (See Figs. 10 - 14) and References 37, 38, 39).

	Γ	A	λ	Mach No.		Fig. No.
1	0	6.0	1.0	0		10
2	0	5.87	.323	0		11
3	0	5.87	.323	.9		11
4	0	2.56	.323	0		11
5	28.4	5.89	.323	0		12
6	28.4	5.89	.323	.9		12
7	48.4	2.56	.323	0		12
8	52.5	2.31	0.	0	Δ wing	13
9	52.5	2.31	0	.9	Δ wing	13
10	71.4	1.01	0	0		13
11	59	3.5	.25	0		14
12	45	5.8	.25	.8		14
13	45	5.8	.25	0		14

The agreement with Falkner's results appears to be quite remarkable and the only really serious discrepancies occur for wing No.8, i.e., the delta wing and for wing No.13.

A point of particular interest is that the empirical formula agrees better with the Falkner solutions which have been corrected by an auxiliary solution than with the uncorrected Falkner solution.

/Falkner ...

Falkner has introduced this auxiliary solution to allow for the effects at the centre section of a swept wing and it can be seen that it considerably alters his standard 126 vortex 6 point solution.

13. Compressible flow

Using the results of the linear perturbation theory, R. Dickson has shown that a wing in compressible flow A_M, Γ_M, λ, may be represented by a wing in incompressible flow A_o, Γ_o, λ, where -

$$A_o = \sqrt{1 - M^2}\ A_M \quad \text{and} \quad \tan \Gamma_o = \frac{\tan \Gamma_M}{\sqrt{1 - M^2}} . \qquad \ldots\ldots\ldots (17)$$

Substituting in the formula for $\bar{y}$, we have

$$\bar{y} = .42 + \frac{A_M}{10^3} \left[(4.4 + 5\ ) \tan \Gamma_M + (10.4\lambda^{\frac{1}{2}} - 6.7)\sqrt{1-M^2}\ \right] \qquad \ldots\ldots\ldots (18)$$

and from this the position of $\bar{y}$ and hence the new loading curve may be calculated for any desired value of M below the critical (within the assumptions of the linear perturbation theory).

In his report Dickson[R] suggests that $\bar{y}$ remains constant independent of Mach number. According to the above equation, however, it will be seen that this is only so when

$$(10.4\lambda^{\frac{1}{2}} - 6.7) = 0, \qquad \ldots\ldots\ldots\ldots (19)$$

i.e., when $\lambda = .415$.

Nevertheless, for wings with taper ratios between about .35 and .45 it will be clear that the shape of the loading curve will not be seriously modified by variations of Mach number and in particular there will be no large movement of aerodynamic centre.

Further inspection of the formula suggests that when $\lambda > .415$ increasing Mach number decreases $\bar{y}$ and the aerodynamic centre moves forward. Similarly when $\lambda < .415$ increasing Mach number increases $\bar{y}$ and the aerodynamic centre moves backwards.

/14. Conclusions ...

[R] The wings analysed by Dickson very nearly satisfy (19).

14. Conclusions

1. The method evolved applies to the additional loading of non-yawed straight tapered swept back wings at small angles of incidence. This limits its use in view of the present trend of swept back wing design (i.e. cranked wings), but it is felt that an extension of the method to cope with these other plan forms should be feasible.

2. The empirical formulae derived for the estimation of $\bar{y}$ and the shape of the non-dimensional loading curve is sufficiently accurate for most practical purposes, both at low speeds and at Mach numbers within the limits of the linear perturbation theory. Any particular case can be estimated in a few minutes.

3. The available data indicates that the accuracy of the empirical formula is better than that of the Weissinger method and comparable with that of the Falkner method, but until more direct experimental evidence is available this cannot be relied upon unconditionally.

/ TABLE I ...

TABLE I

SLOPES OF $\bar{y} - \Lambda$ CURVES $\left[\frac{\partial \bar{v}}{\partial \Lambda}\right]_{\Gamma,\lambda}$

Γ^o	$\lambda = 0$	$\lambda = .25$	$\lambda = .5$	$\lambda = 1.0$	$\lambda = 1.5$
0	.0069	-.0018	.0008	.0040	.006
5	-	-	.0011	-	-
10	.0072	-	.0018	.0052	.0075
15	-	0	.0026	.0060	-
20	.005	-	.00322	.0067	.0096
30	.0039	.0018	.0045	.0085	.0125
45	.0033	.004	.0075	.0130	.018
60	-	.0082	.0125	.02125	.0275

TABLE II

$\bar{y}$ for 40 wings

λ	Γ	A	Weissinger $\bar{y}$	Empirical Formula $\bar{y}$	Experiment $\bar{y}$
.542	0.9	4.47	.425	.4248*	.433
.442	31	4.66	.44	.4395*	.444
.418	46.4	3.45	.442	.4436	.45
0	45	2.76	.41	.4136	
	45	4.5	.405	.4096	
	20	2.35	.405	.408	
	20	4.4	.395	.3975*	
	20	6.6	.39	.3894	
	30	4.3	.400	.402	
	0	2.1	.400	.406	
	0	5.25	.38	.3848	
.25	30	6	.43	.43045	
	60	2.5	.44	.4407	
	15.5	5.0	.42	.42032	
	0	5.3	.41	.4113	
.5	60	1.5	.44	.4388*	
	60	3.5	.464	.4638*	
	45	1.5	.43	.4311	
	45	4.5	.454	.4535*	
	30	2.5	.43	.4313	
	30	4.5	.44	.4403	
	30	8.0	.454	.4562	
	0	3.5	.4225	.4219*	
	0	7.0	.424	.4239*	
	20	4.8	.436	.4347*	
1.0	60	1.6	.454	.452*	
	60	3.0	.48	.48	
	45	1.7	.44	.4423	
	45	3.35	.464	.4639*	
	45	5.0	.48	.4842	
	45	4.1	.472	.4737	
	30	2.0	.436	.438	
	30	3.9	.454	.455	
	30	6.3	.472	.4774	
	0	2.7	.43	.43	
	0	4.2	.436	.4356*	
	0	5.1	.44	.4389*	
	15	1.9	.43	.4318	
	15	3.5	.44	.4418	
	15	5.5	.454	.4542	

* Indicates where the empirical formula slightly underestimates the Weissinger values.

TABLE III

LOADING COEFFICIENTS K_{η}

η \ y	.41	.42	.43	.44	.454	.464	.48
0	1.37	1.31	1.275	1.19	1.10	1.035	.935
.100	1.34	1.30	1.25	1.185	1.12	1.07	1.0
.200	1.30	1.265	1.225	1.18	1.14	1.105	1.05
.382	1.19	1.17	1.165	1.16	1.15	1.14	1.12
.600	.99	1.0	1.03	1.05	1.08	1.10	1.13
.707	.845	.88	.92	.955	.99	1.045	1.10
.800	.71	.74	.79	.83	.88	.94	1.0
.850	.62	.67	.70	.74	.79	.84	.92
.923	.445	.49	.52	.555	.62	.65	.70
.960	.340	.37	.40	.43	.48	.50	.56

TABLE IV

η	Q_η
0	-6.24
.1	-5.00
.2	-3.64
.383	-0.80
.60	+2.00
.707	+3.64
.8	+4.20
.85	+4.20
.923	+3.64
.96	+3.1

REFERENCES

The following references have been used to check the results of the empirical formulae.-

No.	Author	Title, etc.
Calculation of Loading Distributions		
1	J. Weissinger	The lift distribution of swept-back wings. Dec. 1947. N.A.C.A. Tech. Memo 1120
2	J.A. Shortal and B. Maggin	Effect of sweepback and aspect ratio on longitudinal stability characteristics of wings at low speeds. July, 1946. N.A.C.A. Tech. Note 1093
3	J.C. Sivells and R.H. Neely	Calculation of wing characteristics by lifting line theory using non-linear section line data. April, 1947. N.A.C.A. Tech. Note 1269
4	R.A. Mendelsohn and J.D. Brewer	Comparison between the measured and theoretical span loadings on a moderately swept-forward and a moderately swept-back semispan wing. July, 1947. N.A.C.A. Tech. Note 1351
5	N.H. Van Dorn and J. DeYoung	A comparison of three theoretical methods of calculating span load distribution on swept wings. November, 1947. N.A.C.A. Tech. Note 1476
6	J. DeYoung	Theoretical additional span loading characteristics of wings with arbitrary sweep, aspect ratio and taper ratio. Dec. 1947 N.A.C.A. Tech. Note 1491
7	B.H. Wick	Chordwise and spanwise loadings measured at low speed on a triangular wing having an aspect ratio of two and an N.A.C.A. 0012 airfoil section. June, 1948. N.A.C.A. Tech. Note 1650
8	H... Murray	Comparison with experiment of several methods of predicting the lift of wings in subsonic compressible flow. October 1948. N.A.C.A. Tech. Note 1739
9	V.I. Stevens	Theoretical basic span loading characteristics of wings with arbitrary sweep, aspect ratio and taper ratio. Dec. 1948. N.A.C.A. Tech. Note 1772

/10 .

No.	Author	Title, etc.
10	J.D. Bird	Some theoretical low-speed span loading characteristics of swept wings in roll and sideslip. March, 1949. N.A.C.A. Tech. Note 1839
11	D. Cohen	A method for determining the camber and twist of a surface to support a given distribution of lift, with applications to the load over a sweptback wing. 1945. N.A.C.A. Tech. Report 826
12	J. Boshor	The determination of span load distribution at high speed by use of high-speed wing-tunnel section data. Feb. 1944. N.A.C.A. A.C.R. 4B22 (A.R.C. 8114).
13	V.M. Falkner	Preliminary notes on aerodynamic centre of swept-back wings. N.P.L. Report Sept. 1944 (unpublished)
14	" "	Further notes on aerodynamic centre of swept-back wings. N.P.L. Report Sept. 1944 (unpublished)
15	" "	Calculation of aerodynamic loading on a swept-back wing. Jan. 1944 A.R.C. 7322 (unpublished)
16	" "	Comparison of simple calculated characteristics of four swept-back wings. Feb. 1944 A.R.C. 7446 (unpublished)
17	" "	A general solution of the problem of loading on wings with discontinuities of incidence. April, 1944 A.R.C. 7629 (unpublished)
18	" "	Calculation of induced cambers on four wings. May, 1944 A.R.C. 7667 (unpublished)
19	" "	Construction of Tables for calculating the aerodynamic loading of wings. May, 1944. A.R.C. 7732 (unpublished)
20	" "	Effect of sweepback on the aerodynamic loading on a 'V' wing. June, 1944 A.R.C. 7786 (unpublished)
21	" "	Characteristics of a sheared 'V' wing. Dec. 1944. A.R.C. 8255 (unpublished)
22	" "	Lifting plane theory of wings with discontinuities of incidence. May, 1945. A.R.C. 8638 (unpublished)
23	" "	Simplification of wing loading calculations by lifting plane theory. A.R.C. 9211 (unpublished)

/24 ...

No.	Author	Title, etc.
24	V.M. Falkner	Calculation of compressibility effects on loading of a swept-back wing. Dec. 1945 A.R.C. 9261 (unpublished)
25	' '	Proposed definition for sweepback. Dec. 1945. A.R.C. 9237 (unpublished)
26	' '	Theoretical work required for the assistance of designers of aircraft with swept-back wings. Feb. 1946 A.R.C. 9409 (unpublished)
27	' '	The use of equivalent slopes in vortex lattice theory. March, 1946 A.R.C. 9446 (to be published as A.R.C. Reports and Memoranda No. 2295)
28	' '	The accuracy of calculations based on vortex lattice theory. May, 1946 A.R.C. 9621 (unpublished)
29	' '	The calculation of aerodynamic loading on surfaces of any shape. 1943 A.R.C. Reports and Memoranda 1910
30	' '	A note on the present position of calculations by vortex lattice theory. May, 1946 A.R.C. 9637 (unpublished)
31	' '	Tables of Multhopp functions for use in vortex lattice theory. Dec. 1946 A.R.C. 10,220 (unpublished)
32	' '	Calculated aerodynamic characteristics of two infinite wings with constant chord. May, 1947. A.R.C. 10,628 (unpublished)
33	' '	The solution of lifting plane problems by vortex lattice theory. Sept. 1947. A.R.C. 10,895 (unpublished)
34	' '	The solution of lifting line theory of problems involving discontinuities. Oct. 1947 A.R.C. 10, 922 (unpublished)
35	' '	Notes on the stalling of swept-back wings. Oct. 1947. A.R.C. 11,009 (unpublished)
36	' '	Tables of Multhopp and other functions for use in lifting line and lifting plane theory. Feb. 1948 A.R.C. 11,234 (unpublished)

/37 ...

No.	Author	Title, etc.
37	V.M. Falkner	Calculated loadings due to incidence of a number of straight and swept-back wings. June 1948. A.R.C. 11,542 (unpublished)
38	' '	A comparison of two methods of calculating wing loading with allowance for compressibility. Nov. 1948 A.R.C. 11,944 (unpublished)
39	' '	Experiments on sweptback and delta wings in R.A.E. high speed tunnel. Feb. 1947 R.A.E. Tech. Memo Aero 47 (VII International Congress of Applied Mechanics)
40	W. Eisenmann	Calculation of spanwise lift distribution on wing. Feb. 1947 Volkenrohde R. and T. 239
41	P. Jordan	High speed swept-back wings. April 1948 Volkenrohde R. and T. 1014
42	W.P. Jones	Lifting plane theory with special reference to Falkner's approximate method and a proposed electrical device for measuring downwash distributions. May, 1946 A.R.C. Reports and Memoranda 2225
43	H. Schlichting and M. Thomas	Calculation of lift distribution of swept wings. Dec. 1947 R.A.E. Report Aero 2236

Wind Tunnel Tests on Swept-Back Wings

44	D.H. Williams, A.H. Bell and E. Smyth	Tests of aerofoil N.A.C.A. 23012 in the compressed air tunnel. 1939 A.R.C. Reports and Memoranda 1898
45	D.H. Williams, A.F. Brown and C.J.W. Miles	Tests on a tapered wing (N.A.C.A. 23012) with and without sweepback in the compressed air tunnel. May 1945 A.R.C. Reports and Memoranda 2151
46	M. Gdaliahu	A summary of the results of some German model tests on wings of small aspect ratio. Nov. 1946 R.A.E. Tech. Note Aero 1767
47	D.H. Williams, A.F. Brown and C.J.W. Miles	Tests on some 'General Aircraft' wings, with and without sweep back in the compressed air tunnel. Jan 1946 A.R.C. 9321 (unpublished)
48	B. Regenscheit	Tests made on rectangular wing with wing tip aileron. Sept. 1946 Volkenrohde R. and T. 223

/49 ...

No.	Author	Title, etc.
49	W. Krüger	Six component measurements on a cranked swept-back wing. Volkenrohde R. and T. Jan.15th, 1946.
50	G. Thiel and J. Weissinger	Six component measurements on straight and 35° swept back trapezoidal wings with and without split flaps. July, 1946. Volkenrohde R. and T. 523 (A.R.C. 11,741)
51	W. Jacobs	Pressure distribution measurements on a yawed swept back wing of constant chord. July, 1946. Volkenrohde R. and T. 431
52	Th. Schwenk	Measurements on trapezoidal swept back wings. July, 1946 Volkenrohde R. and T. 525
53	H.J. Luckert	Lift distribution on yawed wings. Volkenrohde R. and T. 270
54	Puffert and Bolkow	Three component wind tunnel tests on swept back wings and a complete model. July, 1942 GDC 15/98.T.
55	A.W. Quick	Flight mechanical properties of swept back wings at normal speeds. Apr.1943 Volkenrohde R. and T. 473
56	A. Busemann	Swept back wings at high speeds. Apr.1943 Volkenrohde R. and T. 342

Stability and Control

57	V.M. Falkner and H.L. Nixon	Wind tunnel tests on the stability of two swept-back wings. Oct. 1948 A.R.C. 11,854 (unpublished)
58	H.A. Soule'	Influence of large amounts of wing sweep on stability and control problems of aircraft. June, 1946 N.A.C.A. Tech. Note 1088
59	R.S. Swanson and S.M. Crandall	Lifting-surface-theory aspect-ratio corrections to the lift and hinge-moment parameters for full-span elevators on horizontal tail surfaces. Feb. 1947. N.A.C.A. Tech. Note 1175
60	J.G. Lowry L.E. Schneiter	Investigation at low speed of the longitudinal stability characteristics of a 60° swept back tapered low-drag wing. Aug. .1946. N.A.C.A. Tech. Note 1284

/61 ...

No.	Author	Title, etc.
61	B. Maggin C.V. Bennett	Low-speed stability and damping-in-roll characteristics of some highly swept wings. Nov. 1946 N.A.C.A. Tech. Note 1286
62	" "	Flight tests of an airplane model with a 42° swept-back wing in the Langley free-flight tunnel. Oct. 1946 N.A.C.A. Tech. Note 1287
63	T.A. Toll and M.J. Queijo	Approximate relations and charts for low-speed stability derivatives of swept wings. May 1948 N.A.C.A. Tech. Note 1581
64	W. Letko and J.W. Cowan	Effect of taper ratio on low-speed static and yawing stability derivatives of 45° sweptback wings with aspect ratio of 2.61. July, 1948 N.A.C.A. Tech. Note 1671

Swept-Back Wings with Flaps

65	G. Brennecke	Swept-back wings with counter split flaps. May, 1946. Volkenrohde R. and T. 66
66	W. Krüger	Wind tunnel investigations on 35° swept back wings with different high lift devices. Oct. 1946 Volkenrohde R. and T. 311
67	G. Brennecke	Investigation of sweepback with different high lift devices. Volkenrohde R. and T. 122
68	M. Petkin and B. Maggin	Analysis of factors affecting net lift increment attainable with trailing edge split flaps on tailless airplanes. Sept. 1944 N.A.C.A. A.R.R. L4I18 (A.R.C. 9444)
69	W. Letko and D. Feigenbaum	Wind tunnel investigation of split trailing edge lift and trim flaps on a tapered wing with 23° sweepback. July 1947 N.A.C.A. Tech. Note 1352
70	S. Fischel and M.F. Ivey	Collection of data for lateral control with full span flaps. Apr. 1948 N.A.C.A. Tech. Note 1404
71	G. Lowry and L. Schneiter	Estimation of effectiveness of flap type controls on swept back wings. Aug. 1948. N.A.C.A. Tech. Note 1674

/72 ...

No.	Author	Title, etc.
Induced Drag and Downwash of Swept-Back Wings		
72	V.M. Falkner	The effect of wing twist on the induced drag of sweptback wings. Sept. 1944 A.R.C. 8012 (unpublished)
73	' '	Addendum to 'The effect of wing twist on the induced drag of sweptback wings'. A.R.C. 8012. Oct. 1944 A.R.C. 8137 (unpublished)
74	' '	The calculation by lifting plane theory of the downwash behind a wing. Sept. 1948 A.R.C. 11,778 (unpublished)
75	P.E. Purser, M.L. Spearman and W.R. Bates	Preliminary investigation at low speed of downwash characteristics of small-scale sweptback wings. July 1947 N.A.C.A. Tech. Note 1378
76	S. Katzoff and M.E. Hannah	Calculation of tunnel-induced upwash velocities for swept and yawed wings. Nov. 1948 N.A.C.A. Tech. Note 1748
Miscellaneous		
77	R.T. Jones	Effects of sweepback on boundary layer and separation. July 1947. N.A.C.A. Tech. Note 1402

---oOo---

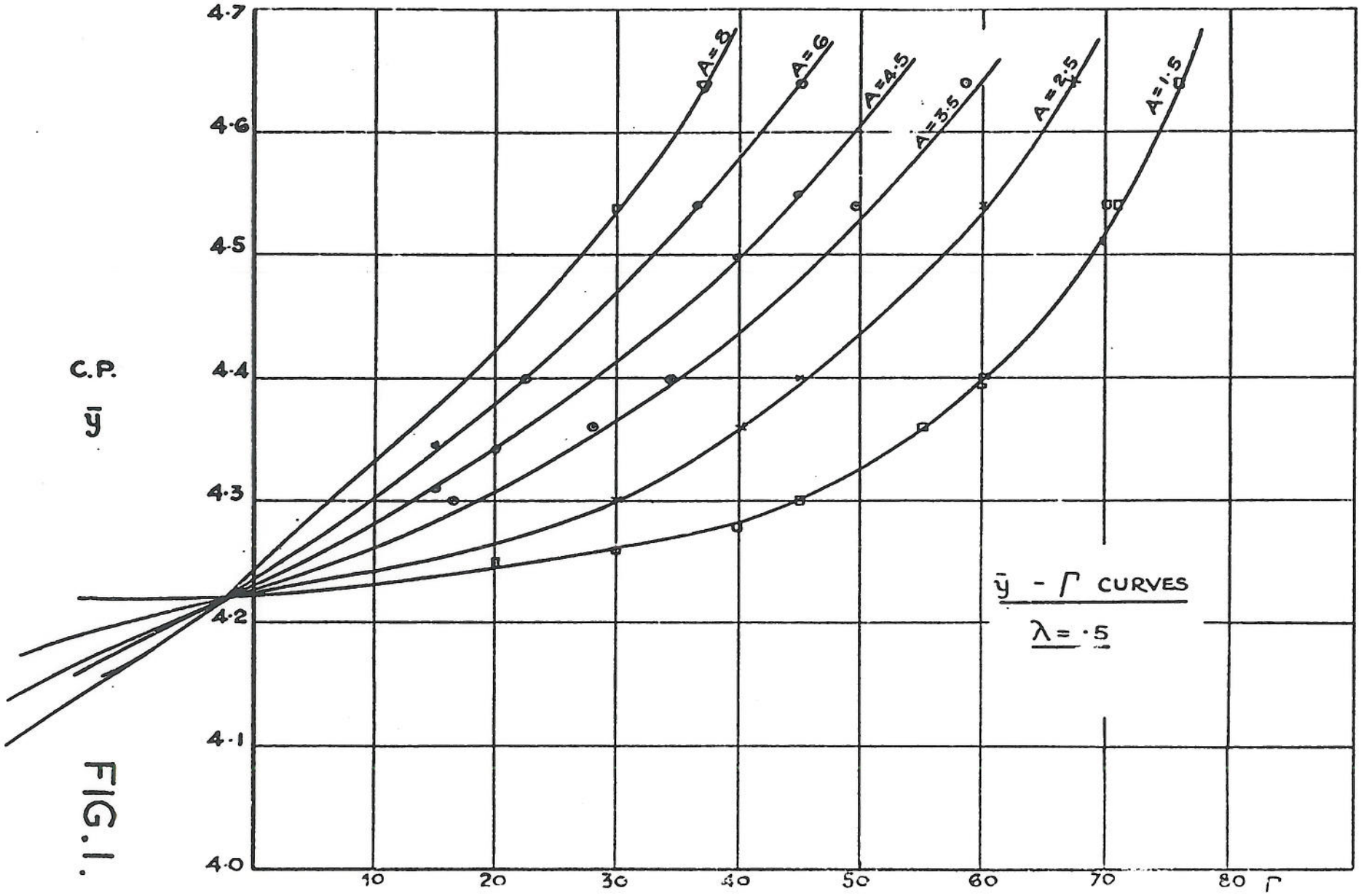
4·7
4·6
4·5
4·4
4·3
4·2
4·1
4·0
C.P.
ȳ
10
20
30
40
50
60
70
80
Γ
A=8
A=6
A=4.5
A=3.5
A=2.5
A=1.5
ȳ - Γ CURVES
λ = ·5

FIG. 1.

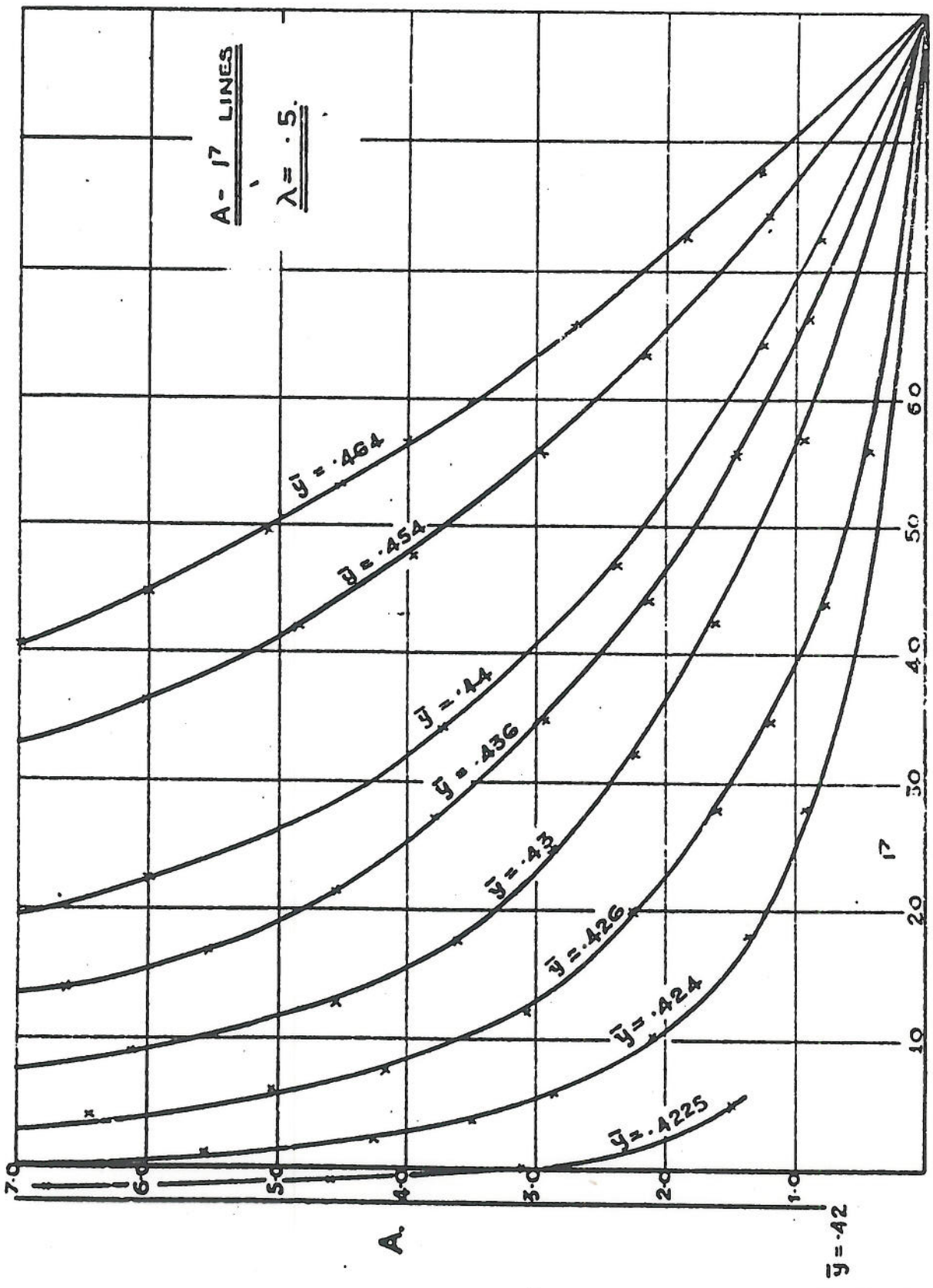
A - I7 LINES
λ = .5.
ȳ = .464
ȳ = .454
ȳ = .44
ȳ = .436
ȳ = .43
ȳ = .426
ȳ = .424
ȳ = .4225
ȳ = .42
I7
A.
7·0
6·0
5·0
4·0
3·0
2·0
1·0
10
20
30
40
50
60

FIG. 2

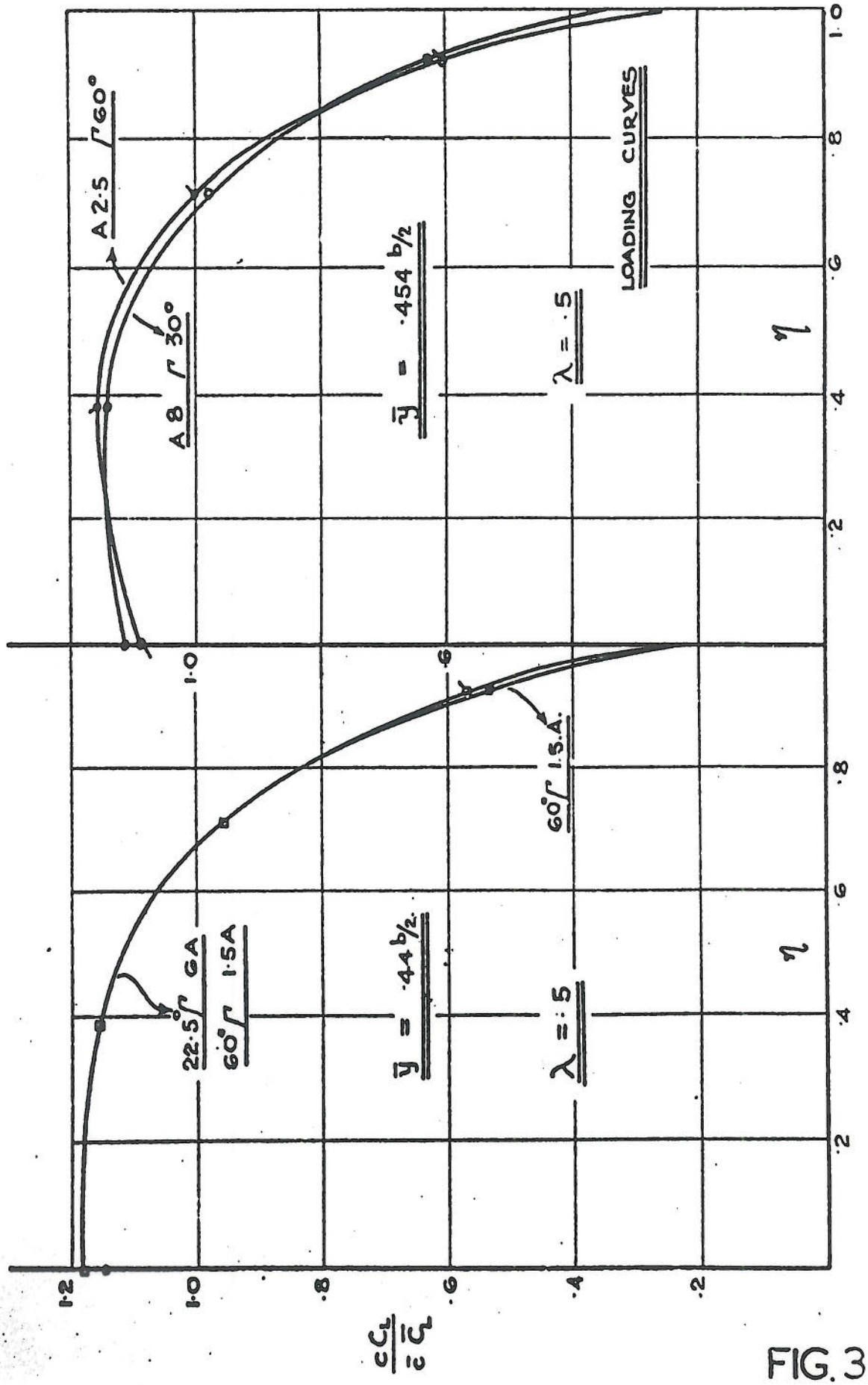
LOADING CURVES
A 2·5 Γ 60°
A 8 Γ 30°
$\bar{y}$ = ·454 b/2
λ = ·5
η
60° Γ 1·5 A.
22·5° Γ 6A
60° Γ 1·5A
$\bar{y}$ = ·44 b/2.
λ = ·5
η
$\frac{c C_L}{\bar{c} \bar{C}_L}$
1·2
1·0
·8
·6
·4
·2

FIG. 3

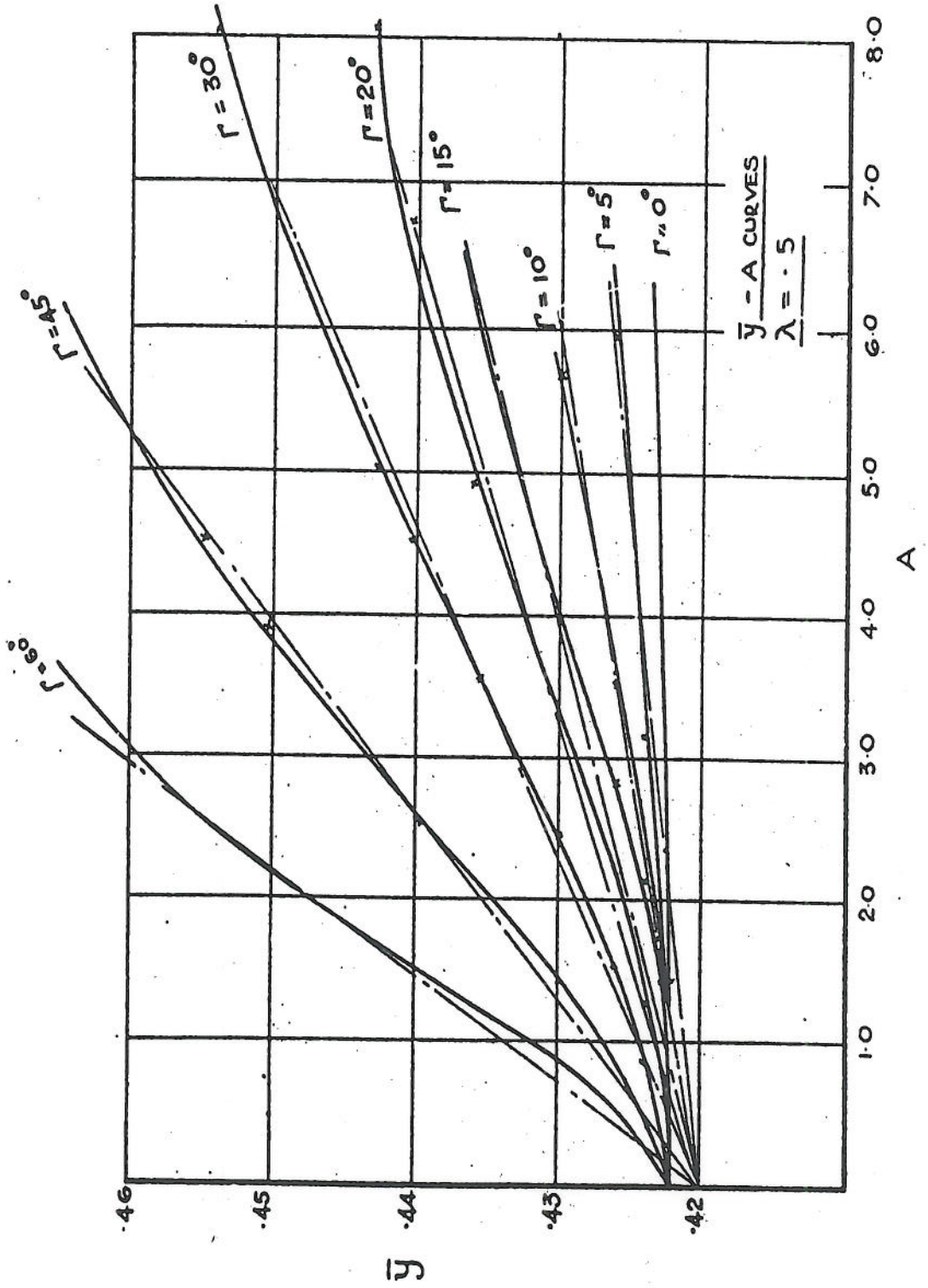
Γ = 30°
Γ = 20°
Γ = 15°
Γ = 10°
Γ = 5°
Γ = 0°
Γ = 45°
Γ = 60°
ȳ - A CURVES
λ = · 5
·46
·45
·44
·43
·42
ȳ
1·0
2·0
3·0
4·0
5·0
6·0
7·0
8·0
A

FIG.4

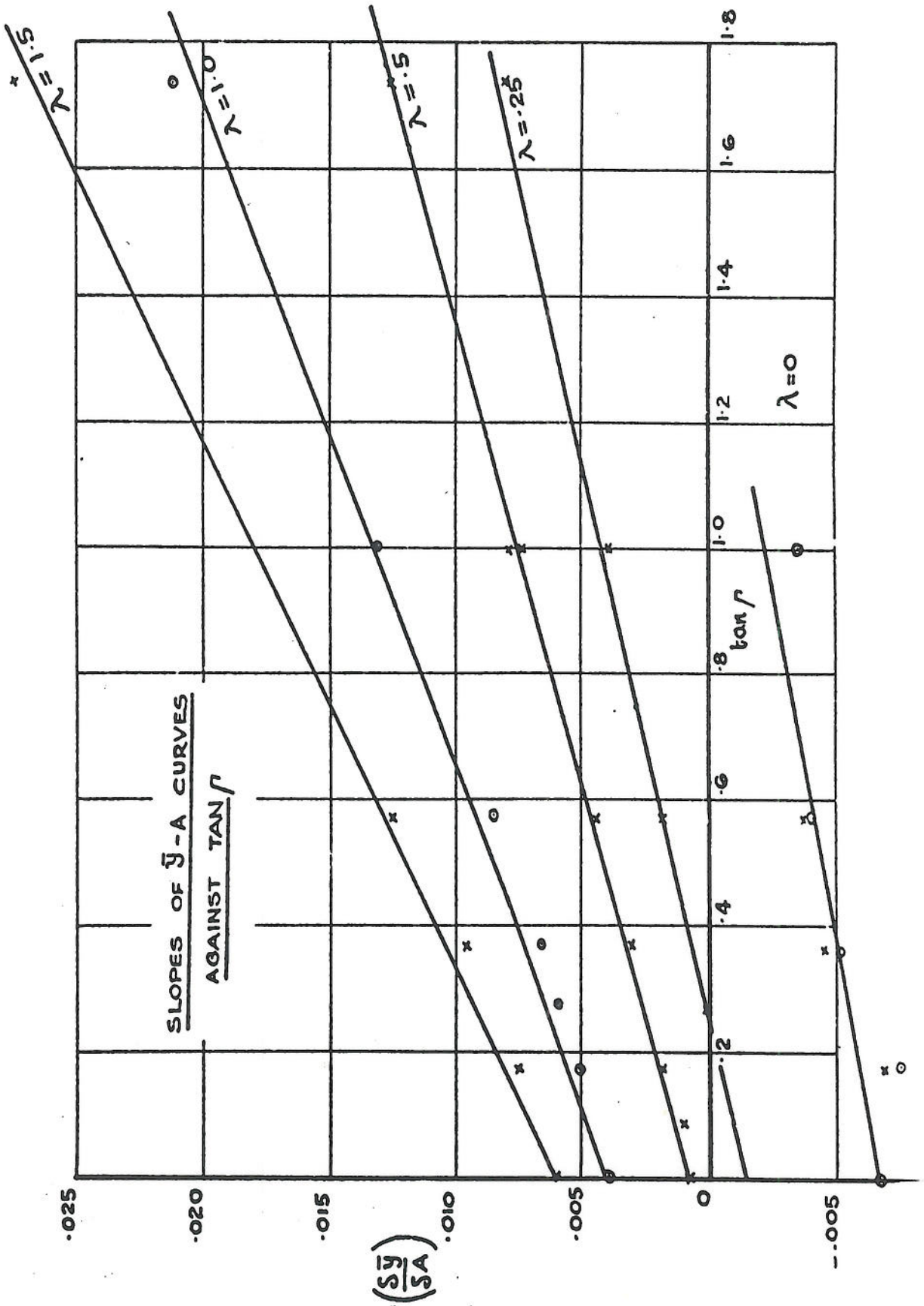
SLOPES OF $\bar{y}$-A CURVES
AGAINST TAN Γ
$\lambda = 1.5$
$\lambda = 1.0$
$\lambda = .5$
$\lambda = .25$
$\lambda = 0$
tan Γ
$\left(\frac{S\bar{y}}{SA}\right)$
.025
.020
.015
.010
.005
0
-.005
.2
.4
.6
.8
1.0
1.2
1.4
1.6
1.8

FIG.5

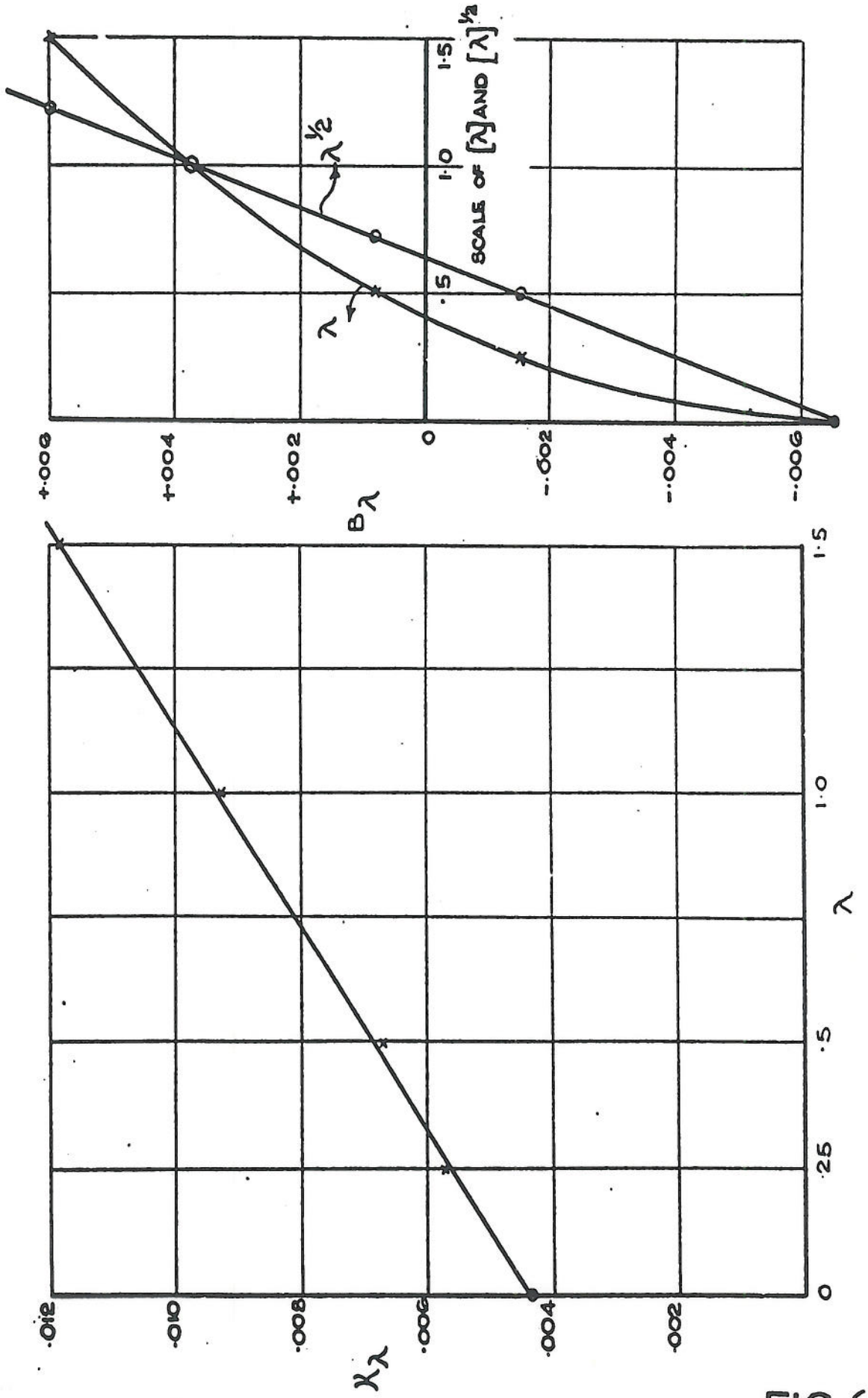
SCALE OF [λ] AND [λ]^½
λ^½
λ
1·5
1·0
·5
+·006
+·004
+·002
0
-·002
-·004
-·006
Bλ
·012
·010
·008
·006
·004
·002
χλ
1·5
1·0
·5
·25
0
λ

FIG.6

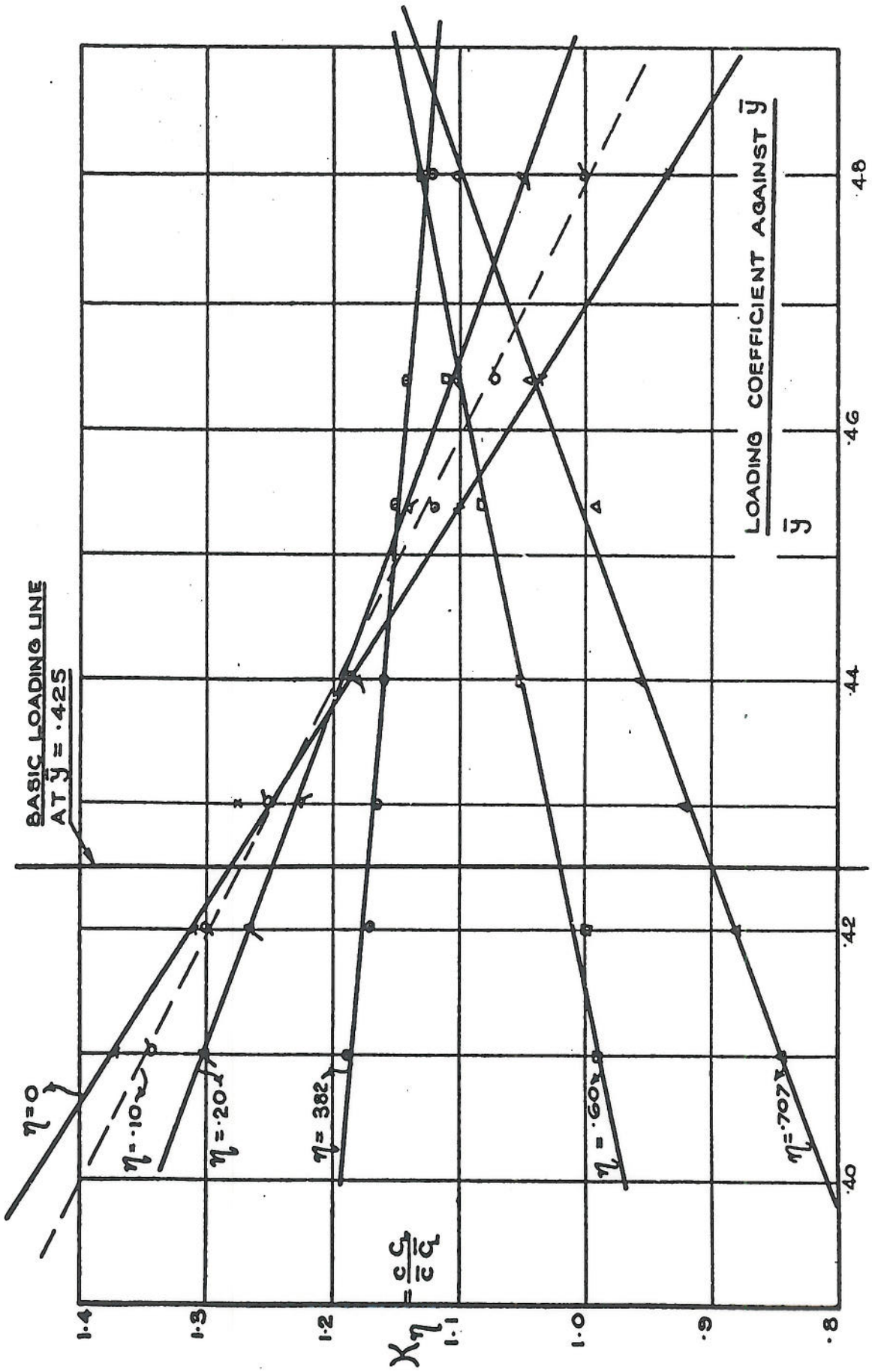
LOADING COEFFICIENT AGAINST $\bar{y}$
$\bar{y}$
BASIC LOADING LINE AT $\bar{y}$ = ·425
η=0
η=·10
η=·20
η= 382
η = ·60
η=·707
$\chi_\eta = \frac{c_{C_L}}{c_{C_L}}$
1·4
1·3
1·2
1·1
1·0
·9
·8
·40
·42
·44
·46
·48

FIG. 7

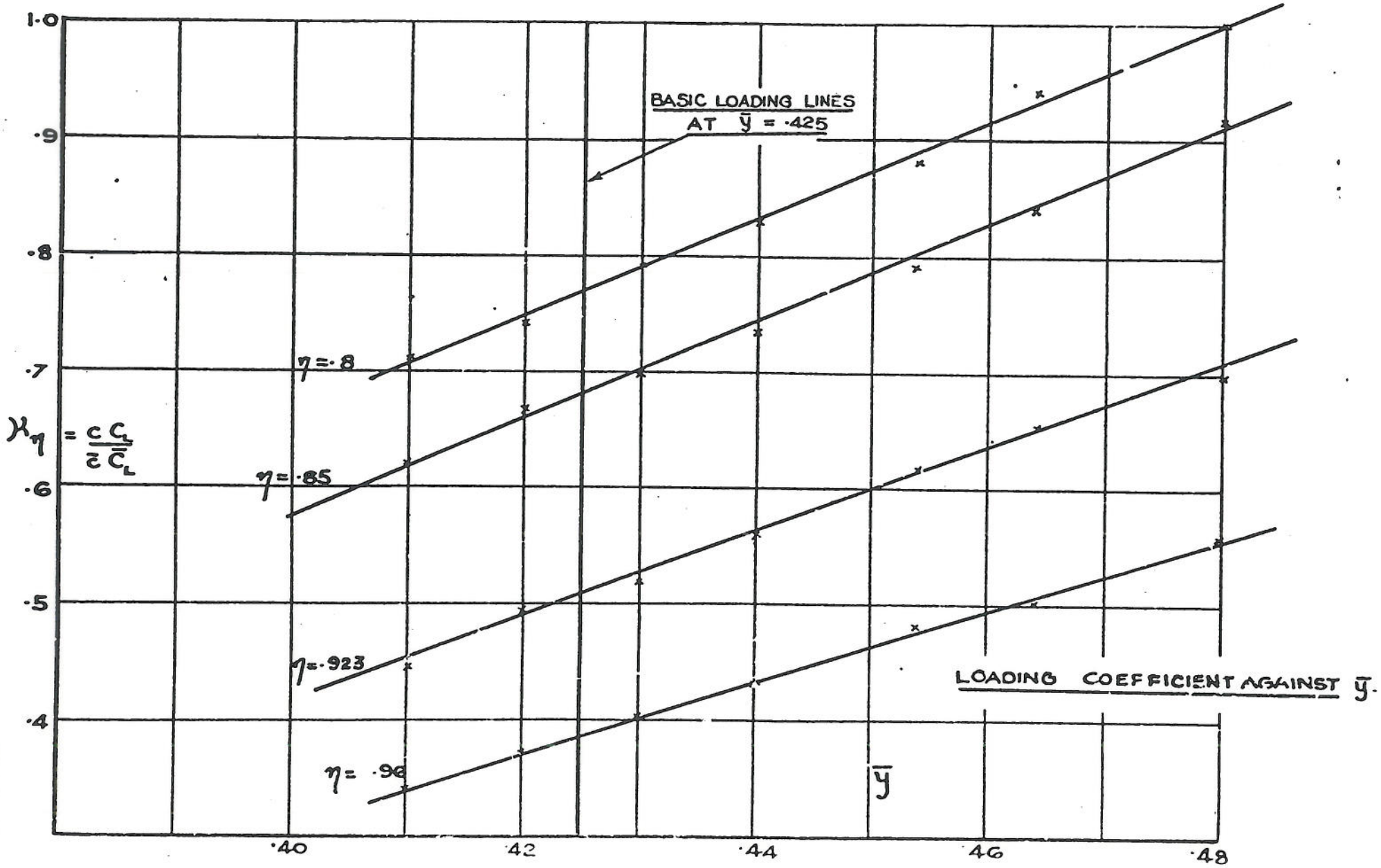

LOADING COEFFICIENT AGAINST $\bar{y}$.

FIG. 8

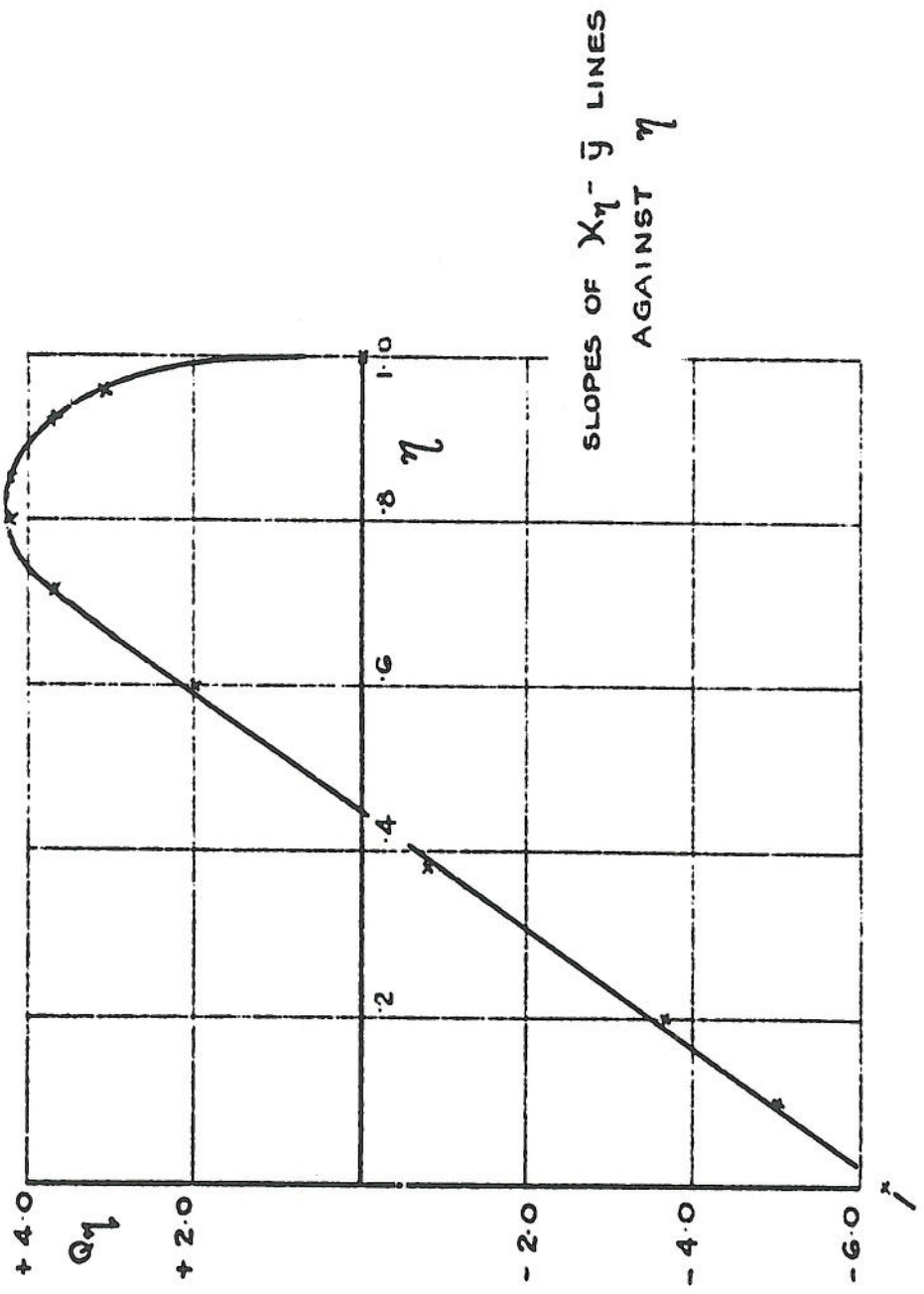
SLOPES OF $X_\eta - \bar{y}$ LINES AGAINST η
η
1·0
·8
·6
·4
·2
Q_η
+4·0
+2·0
-2·0
-4·0
-6·0
i

FIG. 9.

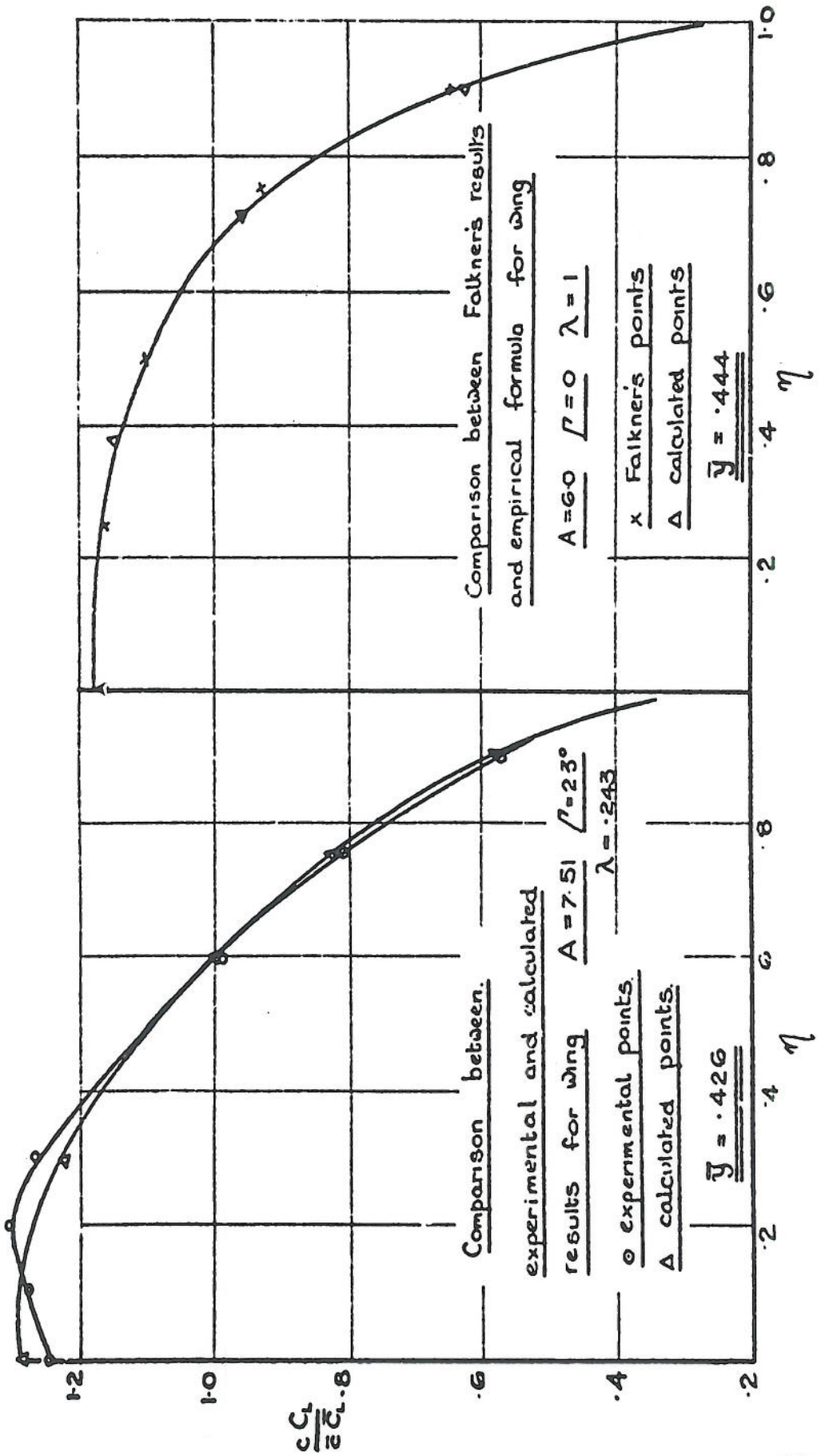
Comparison between Falkner's results and empirical formula for wing
A=6·0 Γ=0 λ=1
x Falkner's points
Δ calculated points
ȳ = ·444
Comparison between.
experimental and calculated results for wing A=7·51 Γ=23° λ=·243
o experimental points.
Δ calculated points.
ȳ = ·426
η
η
$\frac{c C_l}{2\bar{c} C_L}$
1·2
1·0
·8
·6
·4
·2
·2
·4
·6
·8
1·0

FIG. 10

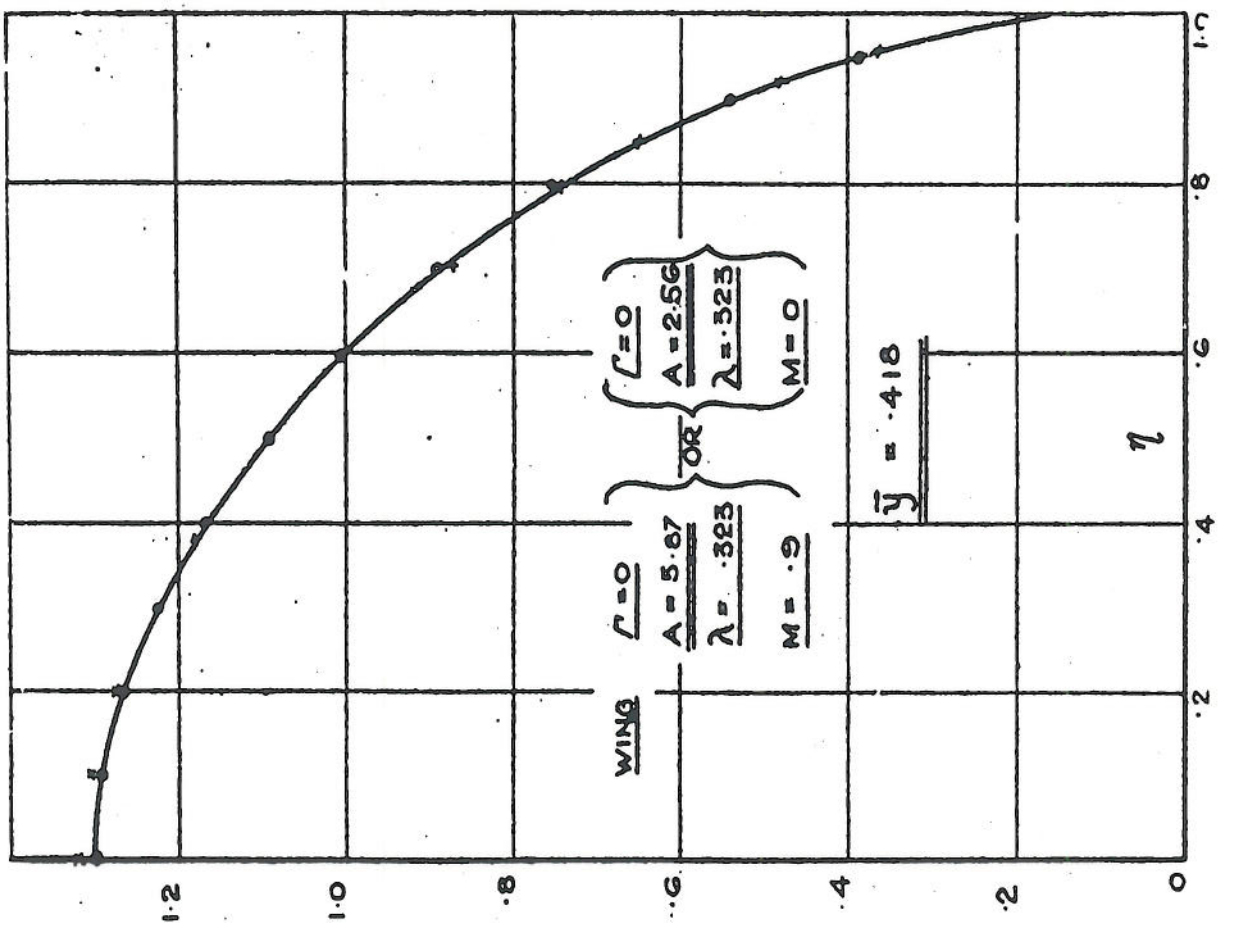

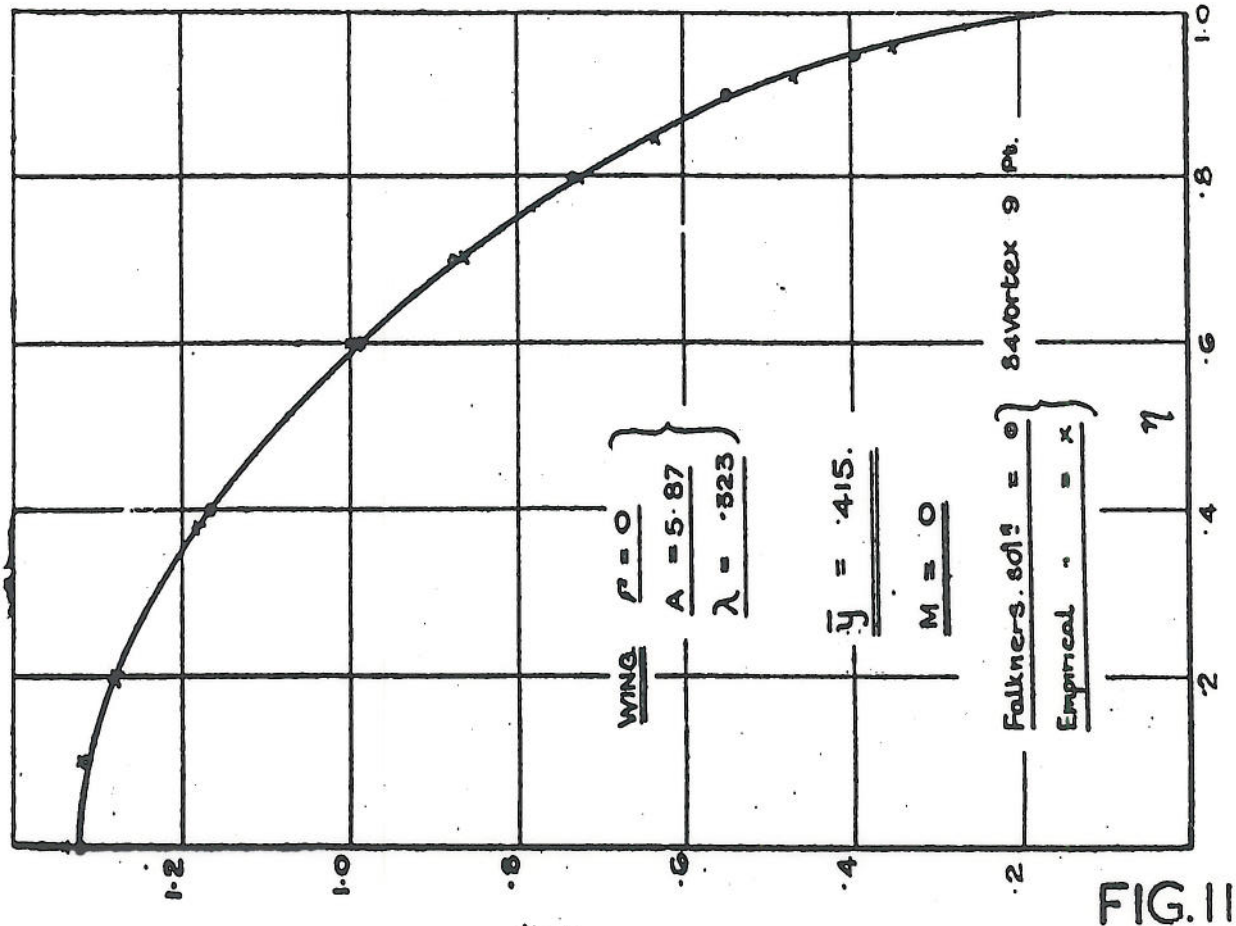

$\frac{c C_l}{2 C_L}$

FIG. 11

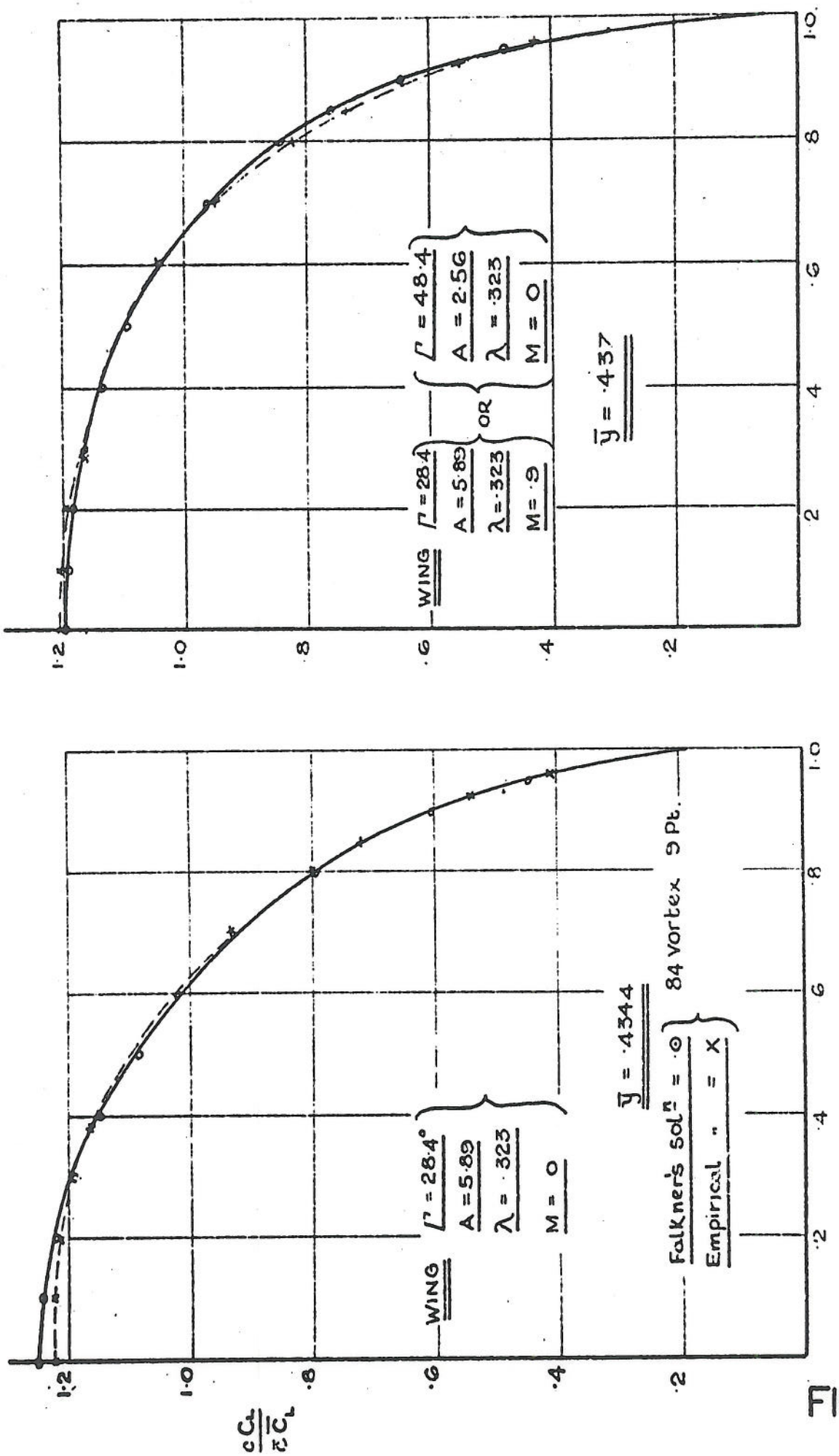
WING
Γ = 28·4°
A = 5·89
λ = ·323
M = 0
ȳ = ·4344
Falkner's sol^{n} = ⊙ 84 vortex 9 Pt.
Empirical " = X
WING
Γ = 28·4
A = 5·89
λ = ·323
M = ·9
OR
Γ = 48·4
A = 2·56
λ = ·323
M = 0
ȳ = ·437
$\frac{c C_l}{\bar{c} C_L}$

FIG.1

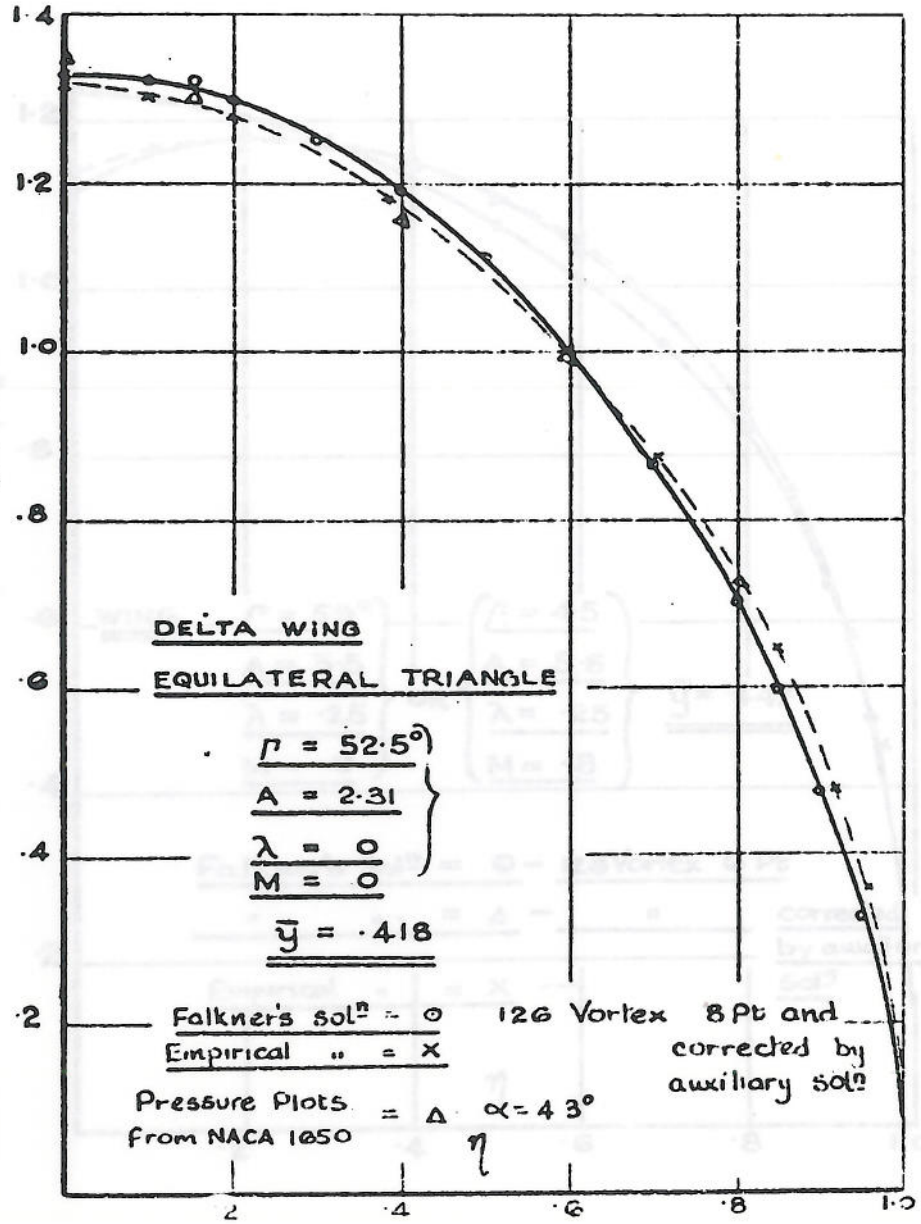
1·4
1·2
1·0
·8
·6
·4
·2
c_p/c_l
DELTA WING
EQUILATERAL TRIANGLE
Γ = 52·5°
A = 2·31
λ = 0
M = 0
ȳ = ·418
Falkner's sol^n = o
Empirical " = x
126 Vortex 8 Pt and corrected by auxiliary sol^n
Pressure Plots from NACA 1050 = Δ α = 4·3°
η
·2
·4
·6
·8
1·0

FIG. 13

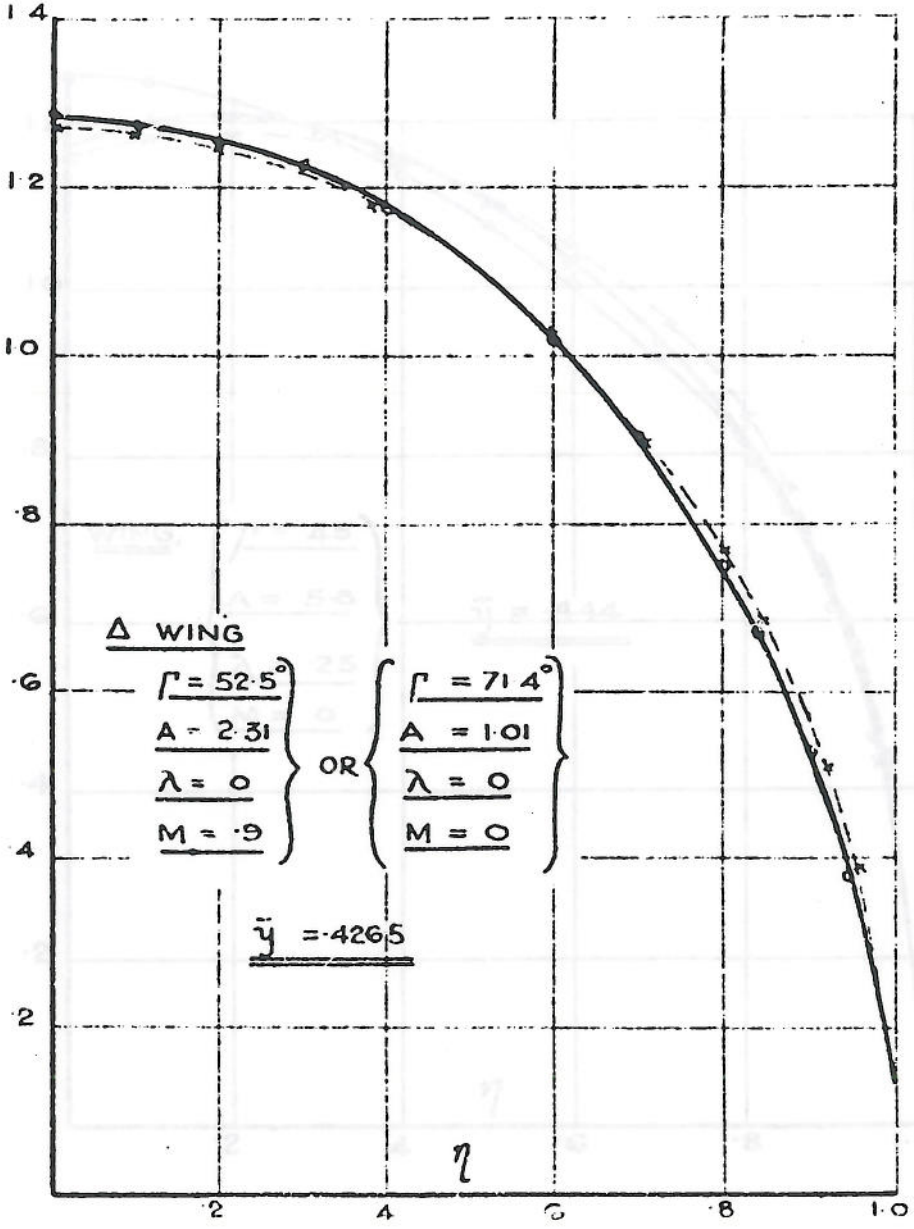
1·4
1·2
1·0
·8
·6
·4
·2
Δ WING
Γ = 52·5°
A = 2·31
λ = 0
M = ·9
OR
Γ = 71·4°
A = 1·01
λ = 0
M = 0
ȳ = ·426·5
η
·2
·4
·6
·8
1·0

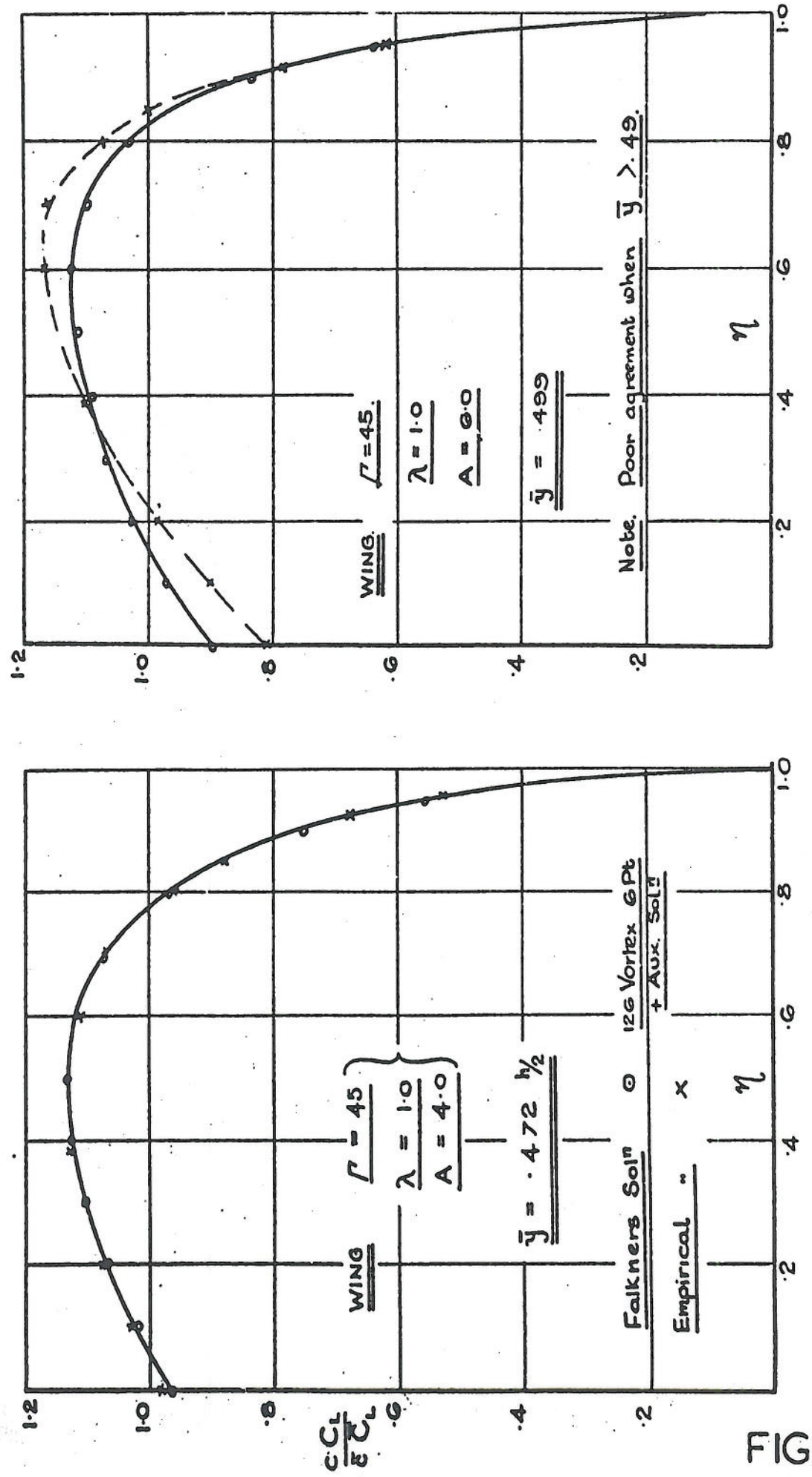
WING
Γ = 45
λ = 1·0
A = 4·0
ȳ = ·472 b/2
Falkners Soln 0 12c Vortex & Pt + Aux. Soln
Empirical " x
η
WING. Γ=45.
λ = 1·0
A = 6·0
ȳ = ·499
Note. Poor agreement when ȳ > .49.
η
c.Cl / ε̄Cl
1·2
1·0
·8
·6
·4
·2

FIG.15

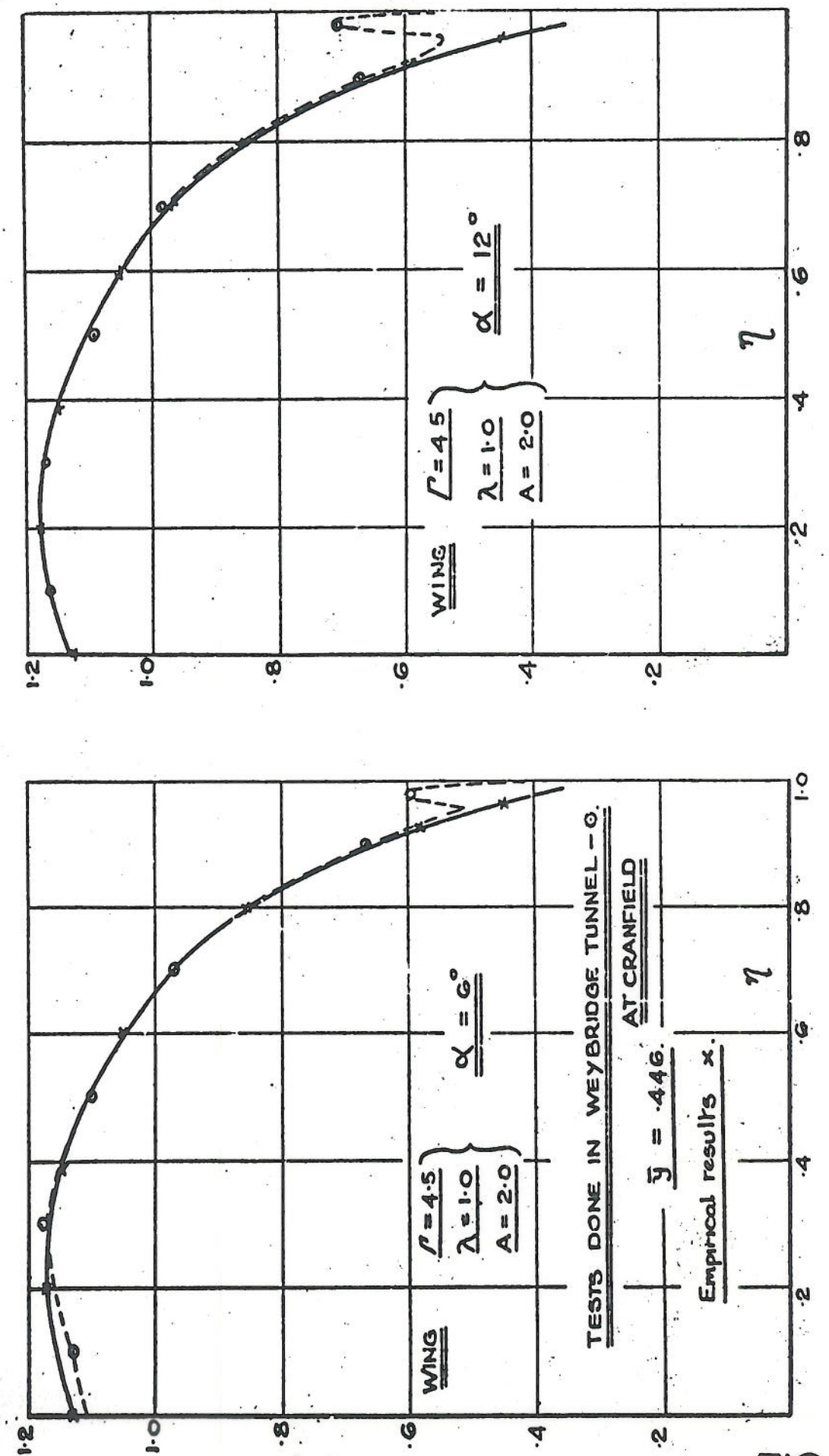
WING
Γ=4·5
λ=1·0
A=2·0
α = 12°
η
WING
Γ=4·5
λ=1·0
A=2·0
α = 6°
TESTS DONE IN WEYBRIDGE TUNNEL — O.
AT CRANFIELD
ȳ = ·446.
Empirical results x.
η
$\frac{C_L}{C_{L_0}}$

FIG.